*34th EPS Conference on Plasma Phys. Warsaw, 2 - 6 July 2007 ECA Vol.**31F**, P-2.051 (2007)*

Particles and energy stochastic transport in the RFX-mod reversed field pinch experiment

P. Innocente, A. Canton, R. Lorenzini, D. Terranova, A. Alfier, E. Martines, F. Bonomo, R. Pasqualotto
Consorzio RFX, Associazione EURATOM-ENEA sulla fusione, Padova, Italy

1. Introduction: The origin of particle and energy transport in the RFP devices is commonly associated to the stochastization of the magnetic field in the plasma core and to the electrostatic fluctuations outside the toroidal field reversal radius at the plasma edge. While, based on edge probes measurements, quantitative evaluations of the contribution of the electrostatic transport have been performed at the plasma edge, due to the lack of field measurements in the plasma core few results have been presented on the comparison between the expected stochastic transport and the measured one in the bulk plasma.

In RFX-mod a set of 48x4 external B_r and B_t magnetic probes allows to measure the magnetic perturbations at the plasma boundary. By means of a Newcomb solver code the eigenfunctions of the field perturbations in the core are computed. The eigenfunctions are used to produce (through a line tracing code) a mapping of the internal magnetic field, so that it is possible to evaluate the magnetic diffusivity.

In the paper the magnetic diffusivity is compared to the experimental particle diffusion coefficient and to the thermal conductivity evaluated by a predictive 1-D code simulating the stationary measured density and temperature profiles. The comparison is performed in two RFX-mod representative plasma currents (I_p=0.6 and 1 MA) and with external field error ranging from 1% to 2%.

2. Field line reconstruction code: In RFX-mod the B_r and B_t magnetic field components measured at the shell are used by a model [1] to compute the internal tearing eigenfunctions in toroidal geometry for a force-free plasma with circular cross section. In the model, in order to properly take into account the toroidal geometry, flux co-ordinates (r, ϑ, ϕ) are adopted together with the controvariant representation of the magnetic field via two independent potentials F and Ψ:

$$\mathbf{B} = \nabla F \times \nabla \vartheta - \nabla \Psi \times \nabla \phi$$

The radial coordinate r is the radius of the unperturbed flux surfaces whose centre is shifted on the equatorial plane relatively to the shell centre by the quantity $\Delta(r)$. The poloidal like coordinate, ϑ, is related to the poloidal angle, θ, corrected at the first order by a function of the major radius R, r, θ and $\Delta(r)$.

The two independent potential are Fourier decomposed up to the maximum m and n allowed by the 48x4 measurements:

$$F(r,\vartheta,\phi) = F_0(r) + \sum_{n\neq n,m} f^{m,n}(r) e^{(m\vartheta - n\phi)} \qquad \Psi(r,\vartheta,\phi) = \Psi_0(r) + \sum_{n\neq n,m} \psi^{m,n}(r) e^{(m\vartheta - n\phi)}$$

The model solves a system of Newcomb-like equations in the two independent potentials for

the modes with the same *n*-number, coupled by toroidicity. The controvariant components of the magnetic fields are finally computed by the relations:

$$B^{\vartheta} = \frac{1}{\sqrt{g}}\frac{\partial \Psi}{\partial r}, \qquad B^{\phi} = \frac{1}{\sqrt{g}}\frac{\partial F}{\partial r}, \qquad b^{r} = -\frac{1}{\sqrt{g}}\left(\frac{\partial F}{\partial r} + \frac{\partial \Psi}{\partial r}\right)$$

where g is metric tensor $1/\sqrt{g} = \nabla r \times \nabla \vartheta \cdot \nabla \phi$.

Starting from the internal tearing eigenfunctions we developed a Field Line Tracing code (FLiT). We preserved in the computation of the internal field line trajectory the toroidal geometry solving the field line equation in the same flux co-ordinates. In these co-ordinates the field line trajectories have been computed integrating the field line equations in the controvariant components:

$$dr = \nabla r \cdot \frac{\mathbf{B}}{|\mathbf{B}|} dl = \frac{B^{r}}{|\mathbf{B}|} dl, \qquad d\vartheta = \nabla \vartheta \cdot \frac{\mathbf{B}}{|\mathbf{B}|} dl = \frac{B^{\vartheta}}{|\mathbf{B}|} dl, \qquad d\phi = \nabla \phi \cdot \frac{\mathbf{B}}{|\mathbf{B}|} dl = \frac{B^{\phi}}{|\mathbf{B}|} dl.$$

In the previous equations the module of the magnetic field |**B**| is computed considering the metric of the toroidal co-ordinates:

$$|\mathbf{B}| = \sqrt{g_{rr}B^{r}B^{r} + g_{\vartheta\vartheta}B^{\vartheta}B^{\vartheta} + g_{\phi\phi}B^{\phi}B^{\phi} + 2g_{r\vartheta}B^{\vartheta}B^{r}}$$

To check the ability of the model used to evaluate the internal tearing eigenfunctions and of the field line integration two different comparisons have been performed. First the shape of the last closed magnetic surface (LCMS) computed with FLiT has been compared to that obtained extrapolating the vacuum field measured at the shell to the plasma edge. Then the position and size of the quasi-single helicity (QSH) islands computed from FLiT has been compared to those deduced from SXR tomography [2]. Figure 1 shows the agreement between the magnetic field surface described by the trajectory of the field line tangent to the first wall and the LCMS deduced from external fields. It has to be noted that although the LCMS has been deduced from the same set of 48x4 magnetic probes the evaluation was validated in the past comparing it with other measurements influenced by the LCMS shape, like the thermal increase of the first wall and the H_{α} emission [3].

Figure 2a shows the thermal island measured from the SXR tomography; the presence of the island is confirmed also by the Thomson Scattering measurements. The FLiT at the same toroidal position of the SXR diagnostic doesn't predict a magnetic island with completely conserved magnetic surfaces but a region of reduced magnetic stochasticity. Figure 2b shows the probability of the magnetic lines starting at the poloidal section of SXR to fill the section (r, ϕ), a lower probability means a lower fields stochasticity. The low chaotic region agrees both in position and size with the thermal island.

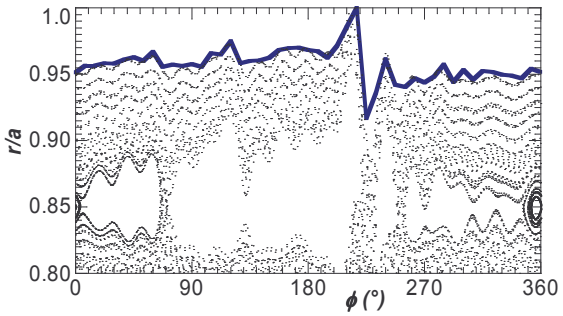

Figure 1. Poincare plot of the field line trajectories and position of the LCMS on the equatorial plane.

3. Transport study: To verify the ability of the stochastic diffusion to describe the RFP transport, the energy and particle transport have been studied and the obtained diffusion coefficients have been compared to the magnetic diffusion coefficient. Indeed in the framework of the Rechester-Rosembluth (RR) transport [4] the electron thermal conductivity and particle diffusion coefficient are related to the amplitude of internal radial field by the relations:

$\chi_E = D_M v_{th}^e$, $\quad D = D_M v_{th}^i$,

where D_M is the magnetic diffusivity, v_{th}^e and v_{th}^i are the electron and ion thermal velocities. The previous relations show that in the RR theory the ratio between thermal conductivity and particle diffusivity is: $\chi_E / D = v_{th}^e / v_{th}^e = \sqrt{m_i / m_e}$ which is 42.85 for the RFX-mod hydrogen plasma. The magnetic diffusivity for circular cross section plasma and a stochastic field can be computed from line field trajectory by the relation:

$$D_M(r) = \frac{<\Delta r^2>}{2L}$$

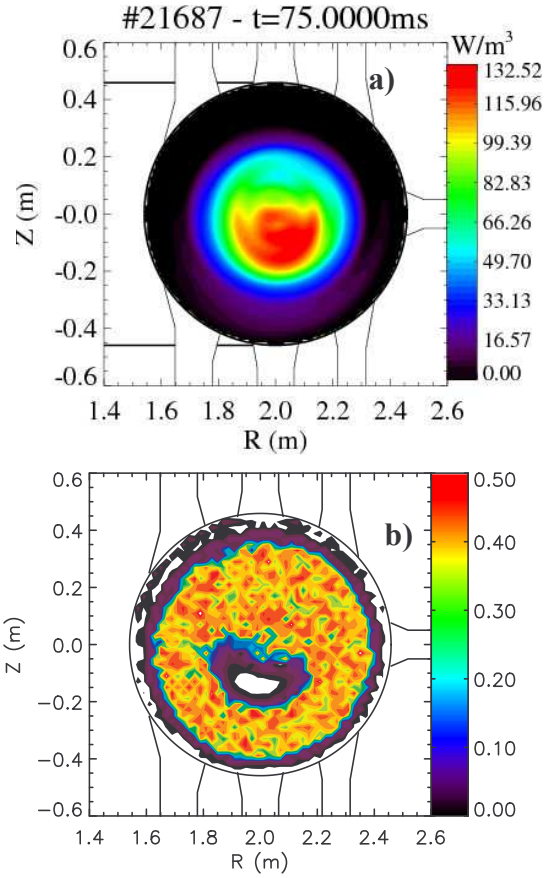

Figure 2. a) Poloidal section of SXR emission; b) Field lines filling probability on the same poloidal section.

where $<\Delta r^2>$ is the ensemble average of the square radial displacement of the field lines starting at the radius *r* after a distance *L*. This relation does not apply in presence of field islands since large radial displacements are possible in presence of conserved (and nearly conserved) flux surfaces.

The experimental thermal conductivity and particle diffusivity are computed solving the 1-D energy and particle transport equations. In the energy equation only the electron contribution to the transport was considered. In the particle transport a convective component due to the ambipolar electric field[5] is included, In the simulations χ_E and D are adapted to minimize the difference between the computed and simulated temperature and density profiles.

An example of computation results is drawn in figure 3 for a good 1 MA discharge with low edge toroidal field error ($b_t/B_p(a)$~1%). Fig. 3c shows that in this case the agreement between the three evaluations of χ_E, $D\sqrt{m_i / m_e}$ and $D_M v_{th}^e$ is good. Different situations exist in which the agreement is worse, for example for a 600 kA with larger field error ($b_t/B_p(a)$~2%) was obtained the result drawn in fig. 4. In this case χ_E is larger than $D\sqrt{m_i / m_e}$ in the core

and smaller in the medium region, the stochastic thermal conductivity is smaller nearly everywhere.

In general the three evaluations agree within a factor of about three in the central region (r/a<0.8). Up to now is not clear whether the observed differences are physically due to some plasma parameter (ie. density or collisionality), or to inaccuracy on diffusion evaluation due measurement errors on density and temperature profiles or particle influx and input power.

In the external region $D_M v_{th}^e$ is usually negligible while the other not, this in agreement with previous studies showing an electrostatic origin of the transport at the edge.

4. Conclusion: By a new field line tracing code the evaluation of the internal tearing eigenfunctions of a previously developed toroidal model has been validated. The internal field line trajectories have been used to compute the stochastic thermal conductivity that was compared to those obtained experimentally and to the particle diffusivity. The results show that the stochastic diffusion can relatively well describe the RFX-mod core energy and particle transport. A statistical analysis underway will try to better verify this result. A different transport mechanism must be present at the edge where stochastic diffusion is negligible.

This work was supported by the European Communities under the contract of Association between EURATOM and ENEA. The views and opinions expressed herein do not necessarily reflect those of European Commission

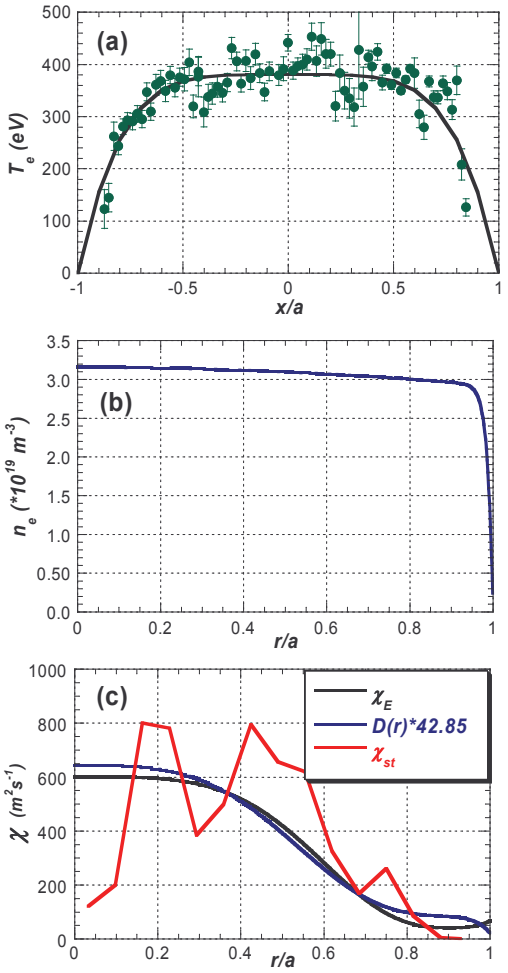

Figure 3. Shot 19700: a) Temperature profile; b) density profile; c) Computed thermal conductivity, scaled particle diffusion and stochastic thermal conductivity.

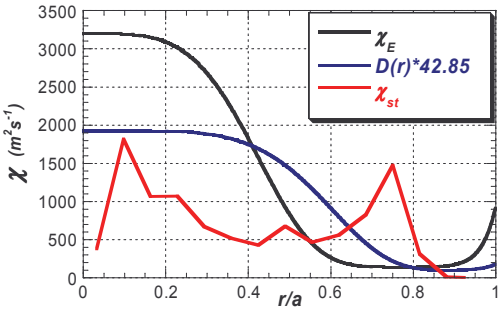

Figure 4. Shot 17884: Computed thermal conductivity, scaled particle diffusion and stochastic thermal conductivity

References:

[1] P. Zanca, D. Terranova Plasma Phys. Control. Fusion 46 (2004) 1115
[2] P. Franz et al., Nucl. Fusion 41, no 6, 695 (2001).
[3] P. Zanca et al. Journal of Nuclear Materials 363-365 (2007) 733-737
[4] A.B. Rechester and M.N. Rosenbluth Phys. Rev. Lett. **40** (1978) 38.
[5] R.W. Harvey, M.G. McCoy, J.Y. Hsu and A.A. Mirin Phys. Rev. Lett. **47** (1981) 102.